Supporting Information (SI)

One-Pot Synthesis to Prepare Lignin/Photoacid Nanohybrid for Multifunctional Biosensor and Photo-Triggered Singlet Oxygen Generation

Ho-Yin TSE[a,b], Chi Shun Yeung[a*], Chun-Yin Lau[a], Man Yee Cheung[c], Jianyu Guan[a], Md Khairul Islam[a], Paul T. Anastas[b*] and Shao-Yuan Leu[a*]

[a] Department of Civil & Environmental Engineering, The Hong Kong Polytechnic University, Hong Kong

[b] School of the Environment, Yale University, USA

[c] School of Biomedical Sciences, The Chinese University of Hong Kong, Hong Kong

[*]Corresponding author: csyeung@polyu.edu.hk

[*]Corresponding author: paul.anastas@yale.edu

[*]Corresponding author: syleu@polyu.edu.hk, Tel: +852-3400-8322

Table Content

Supplementary Figure S7
Corresponding FT-IR spectra of AL-Por-PP-3 after treated with different concentration HSO_3^- ions.

Supplementary Figure S8
UV-vis absorption spectrum of Por-PP at different pH values

Supplementary Figure S9
Fluorescent spectrum of Por-PP at different pH values

Supplementary Figure S10
UV-vis absorption spectrum of AL-Por-PP-1 at different pH values

Supplementary Figure S11
UV-vis absorption spectrum of AL-Por-PP-3 at different concentration of added HSO_3^- ions

Supplementary Figure S12
Heteronuclear single quantum coherence spectroscopy (HSQC) ^1H– ^{13}C spectrum of AL-Por-PP-2

Supplementary Figure S13
Heteronuclear single quantum coherence spectroscopy (HSQC) ^1H– ^{13}C spectrum of AL-Por-PP-3

Reference

Materials

Alkali Lignin (AL) was supplied by Shixian Papermaking in Jilin Province, China. The received lignin was fractionated by different solvent, washed by following order of solvents: hexane, methanol and acetone. The washed AL was extracted by THF. The intention of the organic solvent fractionation is mainly for unifying the quality of the alkali lignin and hence improving the repeatability of the work. The alkali lignin was first washed by hexane to remove low molecular weight apolar components; while the solid residue was washed by methanol to remove small polar components. Acetone was used to remove the soluble lignin oligomers.[1, 2] Finally, the most abundant fraction was utilized in our process, which is the THF dissolved lignin polymer. After the extraction, THF was removed by vacuum evaporation and the AL solid was collected with the mass yield (~72%) as the synthesis raw material in this study. Benzaldehyde, sodium nitrite, 2-phenylphenol, pyrrole, dimethyl sulfoxide, anhydrous tin (II) chloride, nitric acid, hydrochloric acid, propanoic acid, all anion salts mentioned in the article, cysteine, homocysteine and glutathione were analytical grade and purchased from J&K Chemistry Co. Ltd. Deionized Water (resistivity of ≥18 MΩ cm^{-1}) used in our experiments was purified with Millipore water purification system.

Synthesis of meso-tetraphenyl porphyrin (TPP)

Meso-tetraphenyl porphyrin was synthesized using a previously described method with modifications.[3] In a 500 mL three-neck round bottom flask, 4.24 g (40 mmol) of benzaldehyde were dissolved in 200 mL of propanoic acid at 80 °C and the reaction

mixture was magnetically stirred. When the aldehyde was fully dissolved, freshly distilled pyrrole (2.8 mL, 40 mmol) was added to the mixture and brought to reflux for 2 h. The reaction mixture was cooled to room temperature, and then placed in the freezer overnight for porphyrin precipitation. The reaction mixture was vacuum filtered and obtained purple solid was washed with hot deionized water to remove excess acid and water-soluble impurities. The crude product mixture was purified by column chromatography using ethyl acetate with 1% ethanol as the solvent. The purified product yielded a purple solid after reduced pressure rotary evaporation. ^{1}H NMR ($CDCl_3$, 500 MHz) δ: −2.79 (s, 2H, NH), 7.71–7.79 (m, 12H, ArH 8.71–8.23 (m, 8H, ArH), 8.83 (s, 8H, pyrrole-H); MALDI-TOF: calcd for $C_{44}H_{34}N_8$: m/z 614.25, found: 615.29 $[M + H]^+$.

Synthesis of 5,10,15,20-tetrakis(4-nitrophenyl)-porphyrin (TNPP)

The obtained meso-tetraphenyl porphyrin (2g, 3.237 mmol) was placed in a 500 mL 3-neck round bottom flask, and 100 mL of fuming HNO_3 was added dropwise. The reaction was allowed to perform at room temperature & under N_2 atmosphere with stirring for 40 minutes. The reaction was then quenched with aqueous ammonia solution and washed with warm deionized water until the brown powder settled. The crude product was purified by column chromatography on silica gel using ethyl acetate and anisole (9:1) as eluent. The remained reddish-purple band was collected and re-dissolved in ethyl acetate; the remained silica gel was removed by using suction filtration. The purified product was obtained after reduced pressure rotary evaporation. ^{1}H NMR ($CDCl_3$, 500 MHz) δ: −2.82 (s, 2H, NH), 5.53 (s, 8H, amino-H), 8.40 (d, 8H, J = 8.0 Hz, ArH), 8.67 (d, 8H, J = 8.0 Hz, ArH), 8.82 (s, 8H, pyrrole-H); MALDI-TOF: calcd for $C_{44}H_{34}N_8$: m/z 794.19, found: 795.23 $[M + H]^+$.

Synthesis of 5,10,15,20-(2-phenylphenol) 4-azo-porphyrin (Por-PP)

0.22g (0.34mmol) 5,10,15,20-tetrakis(4-aminophenyl)-porphyrin was added to 10mL 1.2M HCl with vigorous stirring in ice-bath for 30 minutes. A solution of sodium nitrite (0.2g, 2mL) was added dropwise and stirred for one hour to prepare the diazonium salt mixture. 0.26g (1.53mmol) of 2-phenylphenol was dissolved in 10 mL 10% NaOH. When the solution was cooled to 0 ^{o}C, it was added dropwise into the diazonium salt mixture for 12 hours reaction in ice-bath. The product was then washed with hot water to remove the salts and the product was purified by column chromatography using ethyl acetate with 10% ethanol as the solvent; the first red color band was collected. The purified product yielded a deep purple solid after reduced pressure rotary evaporation. ^{1}H NMR ($CDCl_3$, 500 MHz) δ: −2.71 (s, 2H, NH), 6.78–8.42 (m, 48H, ArH), 8.95 (s, 8H, pyrrole-H), 13.89 (s, 4H, OH); MALDI-TOF: calcd for $C_{92}H_{62}N_{12}O_4$: m/z 1398.5, found: 1399.5 $[M + H]^{+\cdot}$

Evaluation of excited state pK_a

Analysis based on the Förster cycle[4] is an indirect method used to approximate excited-state acid–base equilibria based on differences in molar enthalpy between the protonated (ROH) and deprotonated (RO^-) species and energies of the 0-0 electronic transitions ($E_{0\text{-}0}$). This method estimates $E_{0\text{-}0}$ as the average of the lowest transition energies measured from the normalized absorption and photoluminescence spectra (λ in nm) as a function of energy.

$$\tilde{v}_{ROH}(cm^{-1}) = \frac{1}{\frac{\lambda_{ROH}^{abs} + \lambda_{ROH}^{PL}}{2}} \times 1e^{7}$$

$$\tilde{v}_{RO^-}(cm^{-1}) = \frac{1}{\frac{\lambda_{RO^-}^{abs} + \lambda_{RO^-}^{PL}}{2}} \times 1e^{7}$$

Cytotoxicity assay

HeLa cells were seeded in a 96-well plate (1×10^4 cells/well) and cultivated in DMEM supplemented with 10% FBS and 1% PS. The cells were then incubated at 37 ℃ in an atmosphere containing 5% CO_2 for 24 h. After 24 h incubation, culture medium in 96-well plate was removed and the HeLa cells were gently washed with PBS. Then, fresh culture medium containing **AL-Por-PP-3** at various concentrations (0, 15, 30, 60, 90, 180 and 360 μg/mL) was added into 96-well plate and incubated for another 24h. After incubation, nanoparticle-containing culture medium was removed and washed with PBS to remove remaining **AL-Por-PP-3**. Pre-warmed fresh culture medium and 20 μL of MTT solution (5 mg/mL) was then added to each well and incubated for 4h. Finally, all solution in well was removed and 150 μL of DMSO was pipetted into each well. The 96-well plate was gently agitated to solubilize purple crystals and mix well. The absorbance of the 96-well plate was measured by microplate reader (Molecular Devices SpectraMax i3X Multimode Microplate Reader) to determine cell viability at a wavelength of 550 nm.

Evaluation of singlet oxygen generation

The singlet oxygen generation capacity of **AL-Por-PP-1** was investigated by the selective singlet oxygen trap molecule 1,3-diphenyl-isobenzofuran (**DPBF**) in ethanol. To evaluate the kinetics of singlet oxygen generation, the mixture solution [**AL-Por-PP-1** (10μg/L) + **DPBF** (50μM)] was irradiated by 600 nm LED light (5 mW cm^{-2}), followed by monitoring the absorbance decrease at 414 nm and plotting it as a function of the absorbance *vs* time.

As a quantitative measurement of the singlet oxygen generation, the quantum yield was calculated using methylene blue (**MB**) as reference[5] with following equation:

$$\Phi(S) = \Phi(R)\left[\frac{k(S)}{k(R)}\right]\left[\frac{F(R)}{F(S)}\right]\left[\frac{PF(R)}{PF(S)}\right]$$

Where Φ(S) is the singlet oxygen generation quantum yield of **AL-Por-PP-1**; Φ(R) is the singlet oxygen generation quantum yield of **MB** under the conditions of the study in ethanol which is 0.52; k is the slope of difference in change in absorbance of DPBF (414 nm) along the irradiation time. F is the absorption correction factor, given as $F = 1 - 10^{-OD}$ (OD is optical density at the irradiation wavelength); PF is incident light intensity (photonic flux in mW/cm^2).

To examine the photostability of **AL-PP-Por-1** nanoparticle and the **DPBF** under the

irradiation, the **AL-PP-Por-1** nanoparticle solution and **DPBF** solution were separately irradiated under same light source. The change of UV-Vis absorption intensities at 414 nm were monitoring along time.

Supplementary table 1

Summary the chemical feeding ratio in the synthesis of AL-Por-PPs and isolated mass yield of the AL-Por-PPs

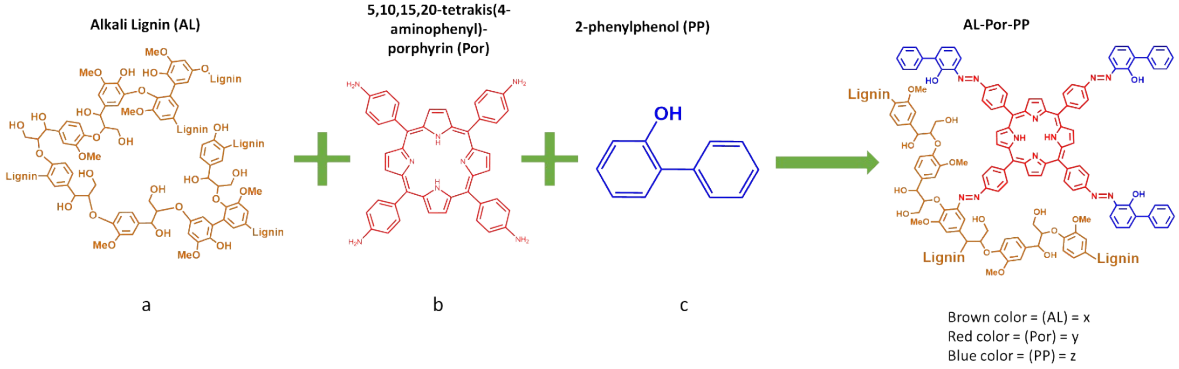

Products	Feed ratio a : b : c (mass %)	Experimental x : y : z (mass %)	Isolated yield
AL-Por-PP-1	0.55 : 0.25 : 0.20	0.59 : 0.23 : 0.18	83 %
AL-Por-PP-2	0.65 : 0.19 : 0.16	0.65 : 0.18 : 0.14	85 %
AL-Por-PP-3	0.75 : 0.14 : 0.11	0.75 : 0.14 : 0.11	86 %

Supplementary table 2

^{31}P NMR spectroscopy characterization of alkali lignin

^{31}P nuclear magnetic resonance (NMR) spectroscopy analysis to characterize the hydroxyl moieties[6] on the **unfractionated alkali lignin & fractionated alkali lignin used for synthesis**:

Moiety	**^{31}P mmol g^{-1}**	
	unfractionated alkali lignin	**fractionated alkali lignin**
Total -OH	5.47	5.22
Aliphatic -OH	1.59	2.30
Total phenolic -OH	3.47	2.64
5-free G unit -OH	1.66	1.05
5-substituted G unit -OH	1.54	1.48
H Unit -OH	0.27	0.11
-COOH	0.41	0.28

The numbers reported above are the mean value of three replicates within =5% of error to the mean.

Supplementary table 3

Gel permeation chromatography (GPC) and zeta potential (ζ) analysis for alkali lignin and AL-Por-PPs

Products	M_w (g.mol^{-1})	M_n (g.mol^{-1})	M_w/M_n	ζ (mv)
Unfractionated AL	5476	846	6.47	-36.8 ± 2.8
Fractionated AL	12582	1418	8.87	-37.4 ± 2.8
AL-Por-PP-1	5782	621	9.31	-38.9 ± 3.5
AL-Por-PP-2	5568	688	8.09	-37.2 ± 3.2
AL-Por-PP-3	5331	747	7.13	-36.3 ± 3.3

Number-average molecular weight (M_n) and weight-average molecular weight (M_w) determined by GPC in THF using PS standards. Zeta potential (ζ) were measured at pH 7. All the numbers reported above are the mean value of three replicates within =10% of error to the mean.

Supplementary table 4

Literature comparison of different HSO_3^- fluorescent probes by structural building block & reagent involved in synthesis, detection range and response time

Probe	Structural building block of the probes	Coupling reagent/catalyst	Detection range	Response Time	Ref.
1	7-(Diethylamino)-2-oxo-2H-chromene-3-carbaldehyde & 1-(1H-benzo[d]imidazol-2-yl) ethanone	Piperidine	1 – 21 µM	10 mins	[7]
2	7-(diethylamino)-3-carbaldehyde-coumarine & d acetophenone	Pyrrolidine & 1,3-dioxolan-2-ylmethyl-triphenylphosphonium bromide	0 – 80 µM	30 mins	[8]
3	4-hydroxycoumarin & cinnamaldehyde	Phosphorus oxychloride & Piperidine	0 – 80 µM	26 mins	[9]
4	2-aminobenzenethiol, 2-hydroxy-3-methylbenzoic acid & 2,3,3-trimethyl-1-(propan-3-sulfonyl) indolenine	Hexamethylenetetramine & Piperidine	0 – 25 µM	5 mins	[10]
5	3-Ethyl-2-methyl-1,3-benzothiazol-3-ium Iodide & 8-hydroxyquino-line-5-carbaldehyde	Piperidine	0 – 10 µM	10 mins	[11]
6	*cis*-Dichlorobis(bipyridine)ruthenium (II), 4-bromo-1,10-phenanthroline, 2,4-dinitroaniline & phenol	Conc. HCl, Sodium nitride & reflux	0 – 70 µM	60 mins	[12]
7	Ruthenium (III) chloride & 4-Methyl-2,2-bipyridyl-4-carboxaldehyde	By reflux	1 – 40 µM	Not given	[13]
This Work	**Alkali lignin, 5,10,15,20-Tetrakis(4-aminophenyl) porphyrin & 2-phenylphenol**	**Conc. HCl & Sodium nitride**	**0 – 20 µM**	**5 mins**	-

Supplementary Figure S1

Porphyrin and 2-phenylphenol moieties content determination by UV-vis absorption and photoluminescence calibration method

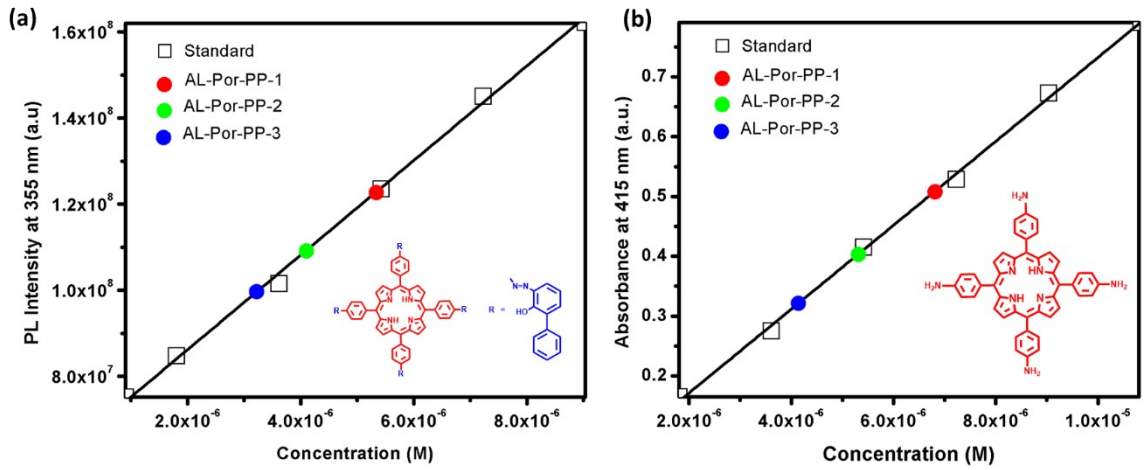

(a) The fluorescent emission of 5,10,15,20-(2-phenylphenol)-(4-aminophenyl)-porphyrin (Por-PP) at 345 nm was recorded in ethanol to calculate the 2-phenylphenol content in AL-Por-PPs.

(b) The absorbance of 5,10,15,20-tetrakis(4-aminophenyl)-porphyrin (TAPP) at 415 nm was measured in ethanol to calculate the porphyrin content in AL-Por-PPs.

Supplementary Figure S2

^{1}H NMR spectroscopy characterization of AL-Por-PP-1

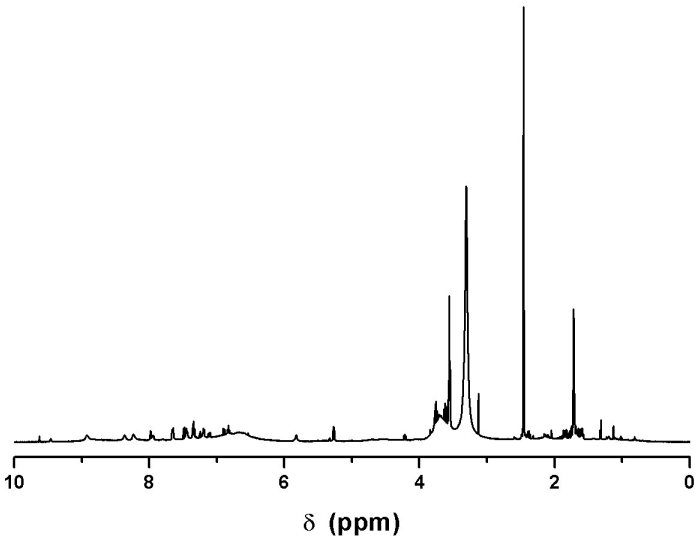

Supplementary Figure S3

^{13}C NMR spectroscopy characterization of AL-Por-PP-1

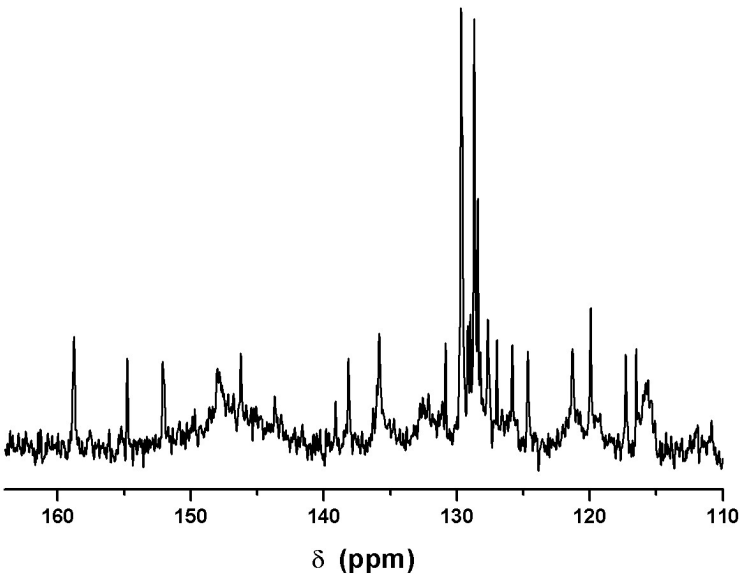

Supplementary Figure S4

Absorption titration of Por-PP to determine the ground-state pKa

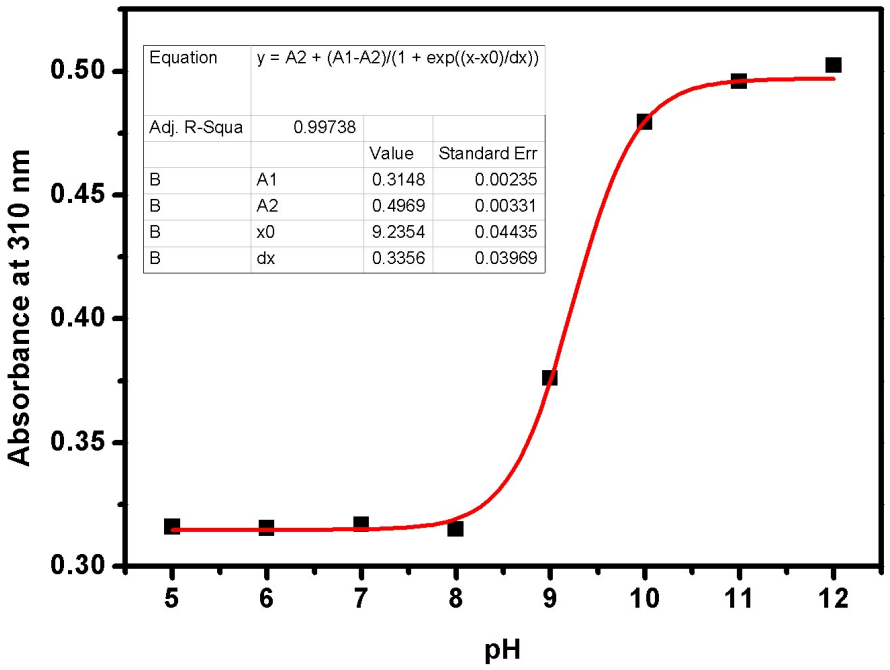

Supplementary Figure S5

Fluorescent titration at 430nm for Por-PP to determine the excited-state pKa

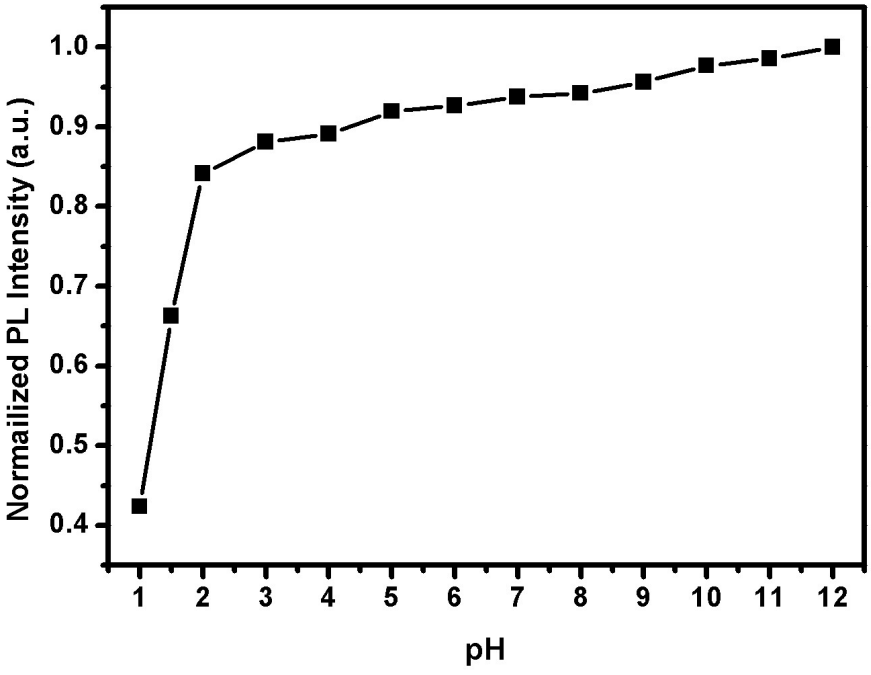

Supplementary Figure S6

The hydrodynamic particle size of AL-Por-PP-3 after addition of different anion ions (25μM) into PBS buffer solution and mixed for 5 minutes

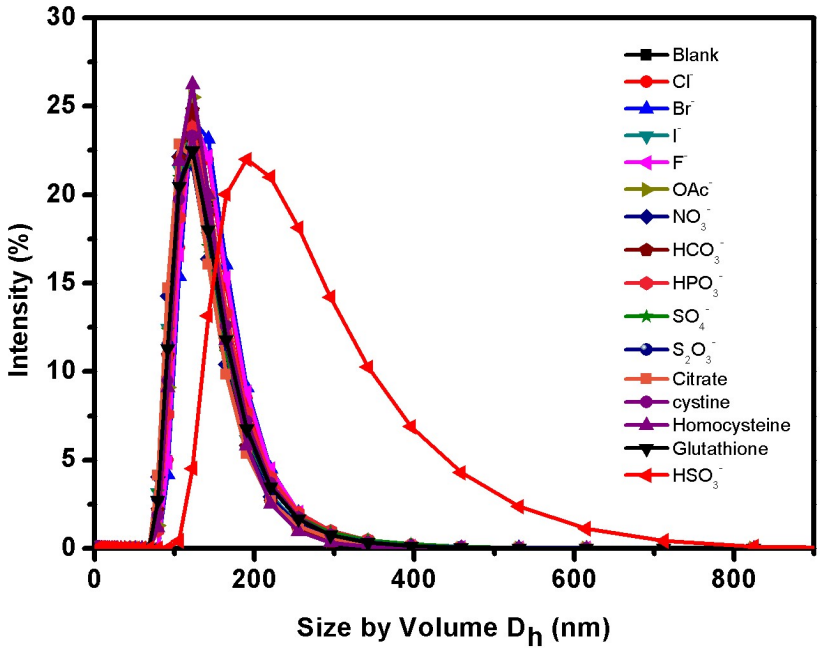

Supplementary Figure S7

Corresponding FT-IR spectrum of AL-Por-PP-3 after treated with different concentration HSO_3^- ions

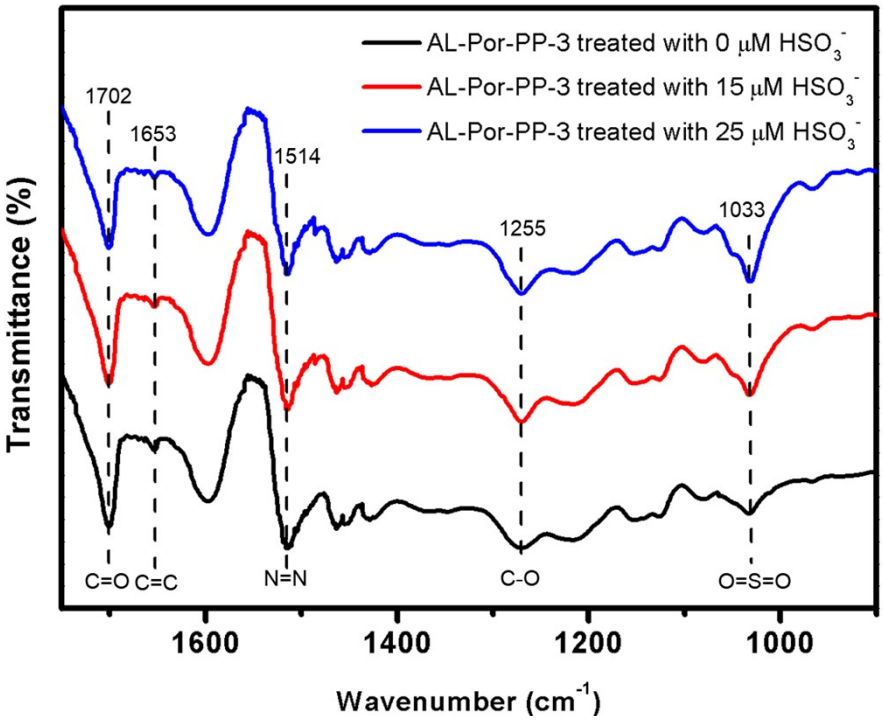

The FT-IR spectrum were collected by the following procedures: 0.1g of AL-Por-PP-3 nanoparticles were mixed with selected concentration HSO_3^- ions in the 10 mL PBS buffer solution (pH=7.4) for 5 minutes to make sure the complete of the addition reaction. The mixed solutions were undergone dialysis with the dialysis tube (4-6k Da) with deionized water to remove the excess HSO_3^- ions for 48 hours. The solvent was then removed by freeze-dry and the reacted AL-Por-PP-3 nanoparticles were collected. The collected sample particles were mixed with the same amount of KBr powder and pressed into the sample disks for the FT-IR measurement.

Supplementary Figure S8

UV-vis absorption spectrum of Por-PP at different pH values

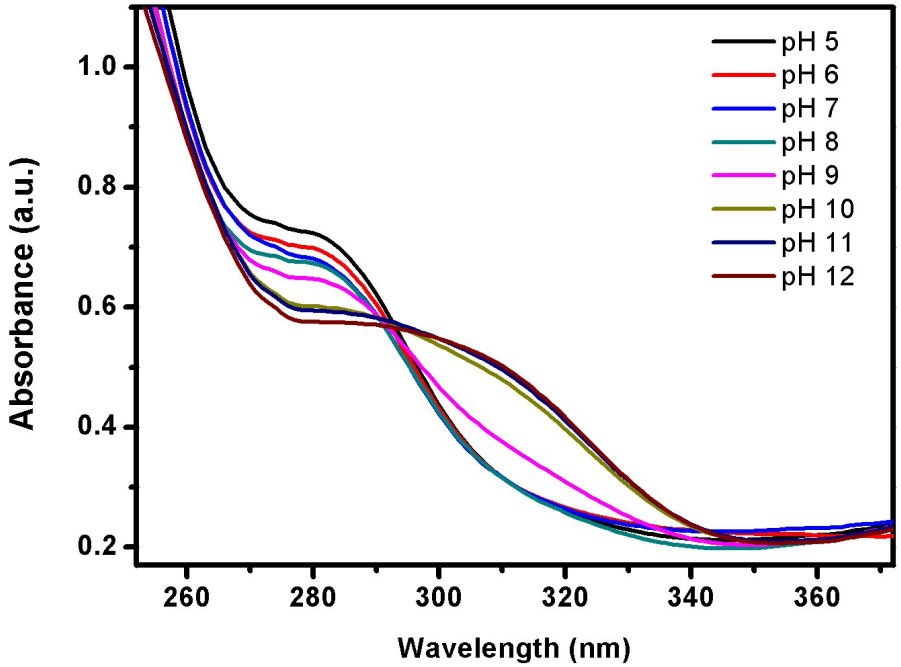

Supplementary Figure S9

Fluorescent spectrum of Por-PP at different pH values

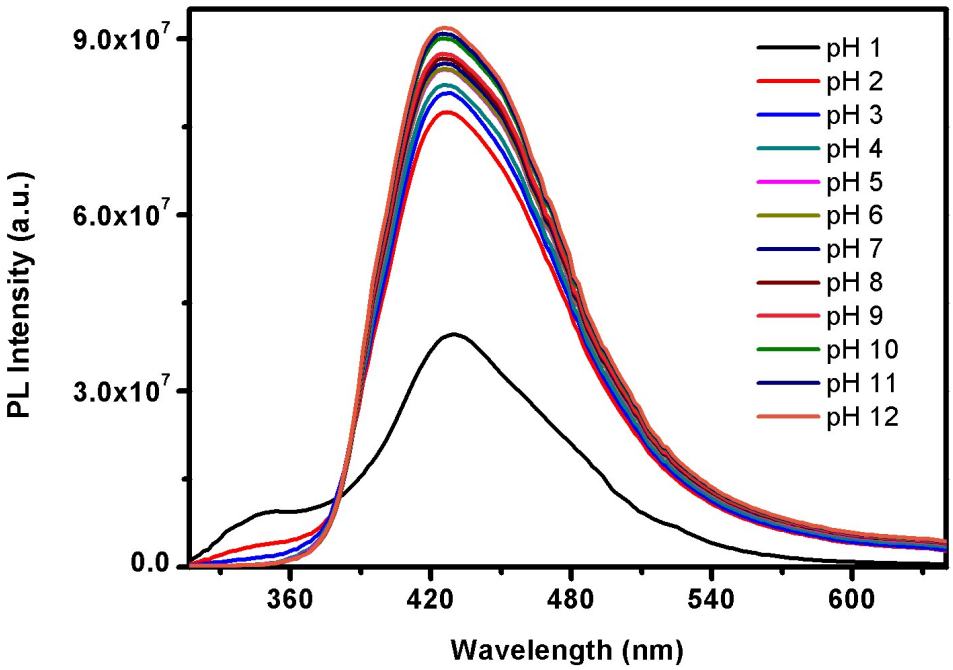

Supplementary Figure S10

UV-vis absorption spectrum of AL-Por-PP-1 at different pH values

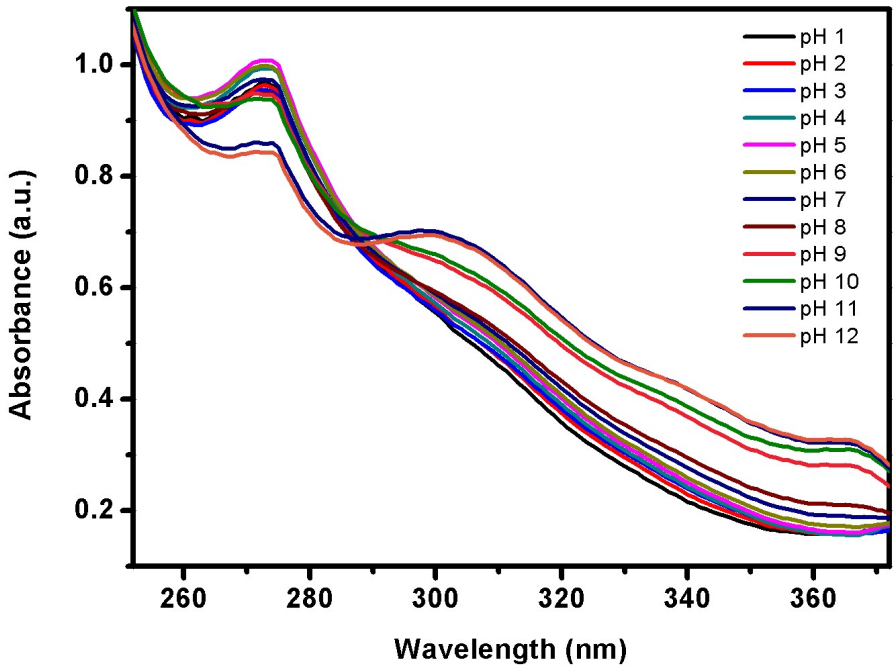

Supplementary Figure S11

UV-vis absorption spectrum of AL-Por-PP-3 at different concentration of added $HSO3^-$ ions

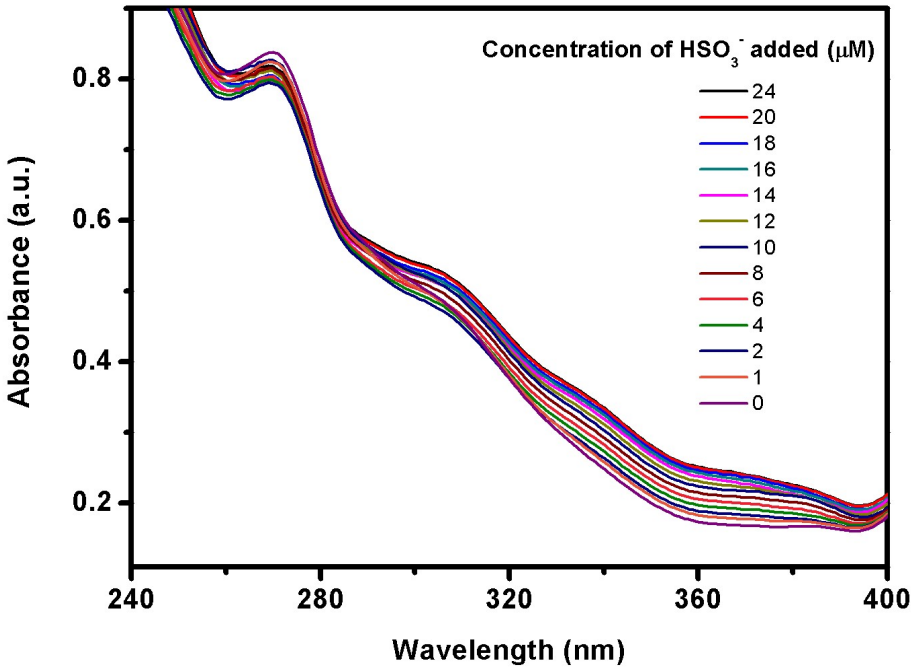

Supplementary Figure S12

Heteronuclear single quantum coherence spectroscopy (HSQC) ^1H– ^{13}C

spectrum of AL-Por-PP-2

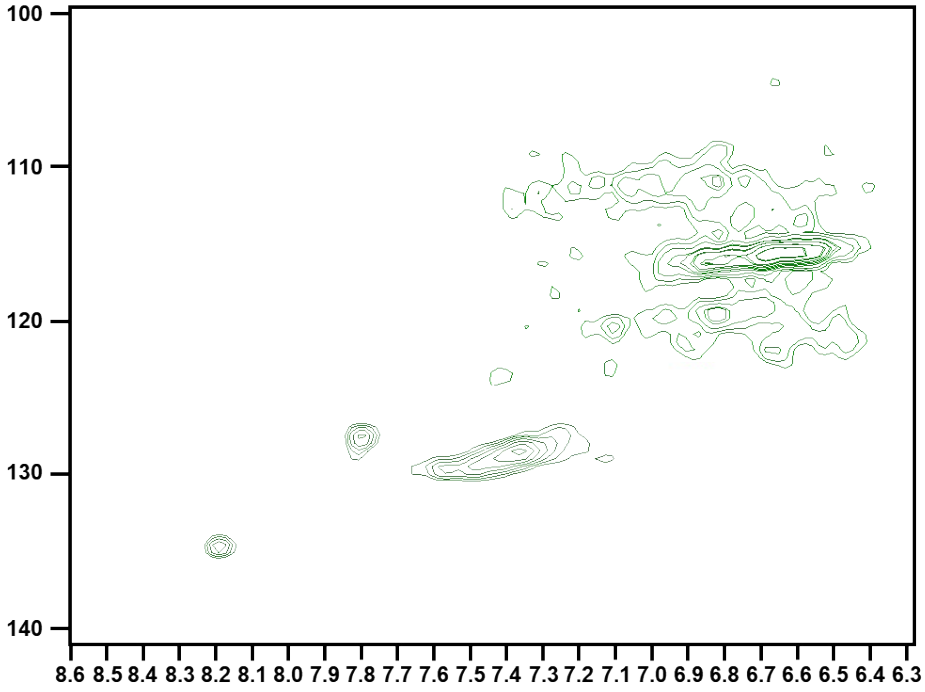

Supplementary Figure S13

Heteronuclear single quantum coherence spectroscopy (HSQC) $^{1}H–^{13}C$ spectrum of AL-Por-PP-3

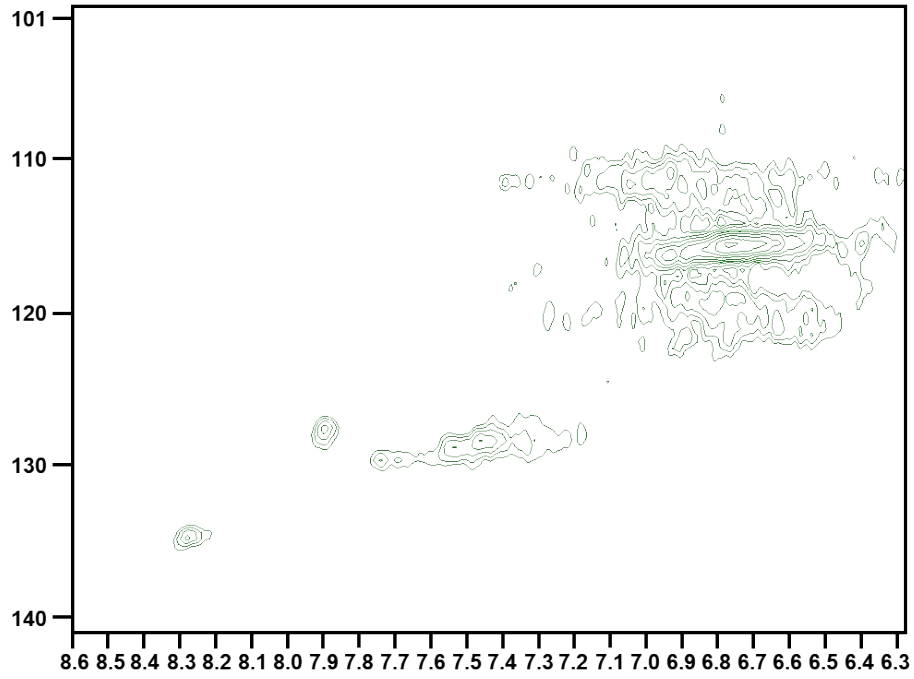

Reference

1. R. E. Majdar, A. Ghasemian, H. Resalati, A. Saraeian, C. Crestini and H. Lange, *Acs Sustain Chem Eng*, 2020, **8**, 16803-16813.
2. N. Giummarella, P. A. Linden, D. Areskogh and M. Lawoko, *Acs Sustain Chem Eng*, 2020, **8**, 1112-1120.
3. P. Rothemund, *J Am Chem Soc*, 1936, **58**, 625-627.
4. B. Marciniak, H. Kozubek and S. Paszyc, *J Chem Educ*, 1992, **69**, 247-249.
5. F. Wilkinson, W. P. Helman and A. B. Ross, *J Phys Chem Ref Data*, 1993, **22**, 113-262.
6. C. Y. Dong, X. Z. Meng, C. S. Yeung, H. Y. Tse, A. J. Ragauskas and S. Y. Leu, *Green Chem*, 2019, **21**, 2788-2800.
7. X. Dai, T. Zhang, Z. F. Du, X. J. Cao, M. Y. Chen, S. W. Hu, J. Y. Miao and B. X. Zhao, *Anal Chim Acta*, 2015, **888**, 138-145.
8. Q. Sun, W. B. Zhang and J. H. Qian, *Talanta*, 2017, **162**, 107-113.
9. J. L. Wang, Y. F. Hao, H. Wang, S. X. Yang, H. Y. Tian, B. G. Sun and Y. G. Liu, *J Agr Food Chem*, 2017, **65**, 2883-2887.
10. H. Y. Zhang, Z. J. Huang and G. Q. Feng, *Anal Chim Acta*, 2016, **920**, 72-79.
11. H. D. Li, *Anal Chim Acta*, 2015, **897**, 102-108.

12. W. Z. Zhang, X. Y. Xi, Y. L. Wang, Z. B. Du, C. L. Liu, J. P. Liu, B. Song, J. L. Yuan and R. Zhang, *Dalton T*, 2020, **49**, 5531-5538.
13. W. Z. Zhang, H. Liu, F. Y. Zhang, Y. L. Wang, B. Song, R. Zhang and J. L. Yuan, *Microchem J*, 2018, **141**, 181-187.